Available online at www.sciencedirect.com

ScienceDirect

Procedia IUTAM 11 (2014) 98 – 109

Procedia IUTAM

www.elsevier.com/locate/procedia

Numerical study of a non-local weakly nonlinear model for a liquid film sheared by a turbulent gas

Te-Sheng Lin[a], Dmitri Tseluiko[a], Serafim Kalliadasis[b]

[a]*Department of Mathematical Sciences, Loughborough University, Loughborough, LE11 3TU, UK*
[b]*Department of Chemical Engineering, Imperial College London, London, SW7 2AZ, UK*

Abstract

We investigate a weakly nonlinear equation that arises in the modelling of wave dynamics on a liquid film flowing down an inclined plane when a turbulent gas flows above it. The model is the Kuramoto-Sivashinsky equation with an additional non-local term multiplied by a parameter representing the relative importance of the turbulent gas. The non-local term has a dispersive effect, destabilising effect on long waves and stabilising or destabilising effect on short waves depending on whether the gas flows downwards or upwards. We investigate the influence of this term on the dynamics of the Kuramoto-Sivashinsky equation by extensive numerical experiments. When the gas parameter is sufficiently large, the solution evolves into a row of weakly interacting pulses.

Selection and peer-review under responsibility of Cyprus University of Technology

Keywords:

1. Introduction

Gas-liquid flows occur both in nature and in numerous technological applications such as chemical reactors, cooling systems and evaporators. Here we consider a liquid film that flows down a lower wall of an inclined channel under the action of gravity and with a counter-current turbulent gas flowing above the liquid film. Counter-current gas-liquid flows have been actively studied both experimentally and theoretically starting from the experiments of Semyonov [1], who analysed counter-current flows of water liquid films and air in glass tubes. He found that such flows are characterised by various interesting phenomena of which the most interesting one is the so-called flooding phenomenon: as the gas flow rate is increased, the amplitude of the interfacial waves grows very rapidly before the complete flow reversal.

Other experimental works on counter-current gas-liquid flows include those in Refs. [2,3,4,5,6,7,8,9,10,11,12,13]. As a result of these studies, there have appeared a number of empirical relations that attempt to express the gas velocity at which flooding occurs as a function of physical properties of the gas and the liquid and the geometrical properties of the channel. Theoretical investigations of flooding include works by Shearer and Davidson [14], Guguchkin *et al.* [15], Demekhin [16], Jurman and McCready [17], Peng *et al.* [18]. Trifonov [19,20,21] used an approach in which, under appropriate conditions, the gas problem can be solved independently of the problem for the liquid film following the studies of Miles [22] and Benjamin [23]. Trifonov then analysed the problem for the liquid film using full Navier-Stokes equations. Recently, Tseluiko and Kalliadasis [24] and Vellingiri *et al.* [25] adopted an approach similar to that of Trifonov, but with a more accurate model for the gas phase (which gives significantly better agreement with

Email addresses: t.lin@lboro.ac.uk (Te-Sheng Lin), d.tseluiko@lboro.ac.uk (Dmitri Tseluiko), s.kalliadasis@imperial.ac.uk (Serafim Kalliadasis)

2210-9838
Selection and peer-review under responsibility of Cyprus University of Technology
doi:10.1016/j.piutam.2014.01.052

experimental studies of e.g. Thorsness *et al.* [26] and Zilker *et al.* [27]) and derived a low-dimensional integral-boundary-layer (IBL) model for the liquid film that is more suitable for a systematic investigation of gas-liquid flows than the full Navier-Stokes equations. The IBL model for a free falling film was first introduced by Shkadov [28] and was improved by Ruyer-Quil and Manneville [29,30,31]. Tseluiko and Kalliadasis [24] and Vellingiri *et al.* [25] extended the approach of Ruyer-Quil and Manneville to two-phase gas-liquid flows. These models have been further extended to include additional complexities, e.g. Marangoni effects [32,33,34,35]. The advantage of IBL models is that they capture accurately the instability onset and they correctly describe nonlinear waves sufficiently far away from the critical Reynolds number.

In the present study, we consider a weakly nonlinear model that is valid in a close neighbourhood of the critical Reynolds number and is derived under the assumption that the amplitude of the interfacial waves is small. The model was derived in Ref. [24]. It is the Kuramoto-Sivashinsky (KS) equation with an additional non-local term that represents the effect of the turbulent gas. This non-local term has a dispersive effect, destabilising effect on long waves and stabilising or destabilising effect on short waves depending on whether the gas flows downwards or upwards. It is well known that the dynamics of the KS equation is chaotic in sufficiently large domains, see e.g. Refs. [36,37,38,39]. On the other hand, it has been shown that dispersion in the form of a third-derivative term has a regularising effect on the chaotic dynamics of the KS equation and the solution evolves into arrays of travelling pulses, see e.g. Refs. [40,41,42]. In the more recent studies of Refs. [43,44,45,46] the regularising effect of dispersion was further analysed and a rigorous coherent-structure theory for solitary pulses' interaction was developed; the theory has also been extended to the free falling film problem. In the present study, we analyse how the regularising dispersive effect and destabilising effect of the non-local 'gas term' affect the dynamics of the KS equation.

The paper is organised as follows. In Sec. 2, we present a summary of the derivation of the weakly nonlinear model for the liquid film in the presence of a turbulent gas. In Sec. 3, we present our numerical results. We conclude in Sec. 4.

2. Summary of model derivation

We outline briefly the derivation of a weakly nonlinear model describing wave evolution on a liquid film sheared by a turbulent gas. For more details see Refs. [24,25].

The main idea in the derivation is that under appropriate conditions the gas-liquid interface can be considered as a solid wall for the gas problem. Therefore, for any prescribed interface profile, one can solve the gas problem independent of the liquid flow. Under such an approach, the shear and normal stresses acting by the turbulent gas on the interface can be expressed in terms of the interface profile, and these stresses will enter the stress balance conditions for the liquid problem. Following the well-known long-wave approach, one can derive the evolution equation of the height of the liquid film. A weakly nonlinear expansion of this equation results in a KS equation with additional non-local terms representing the effect of the turbulent gas.

2.1. Gas problem

The gas flow is modelled by the incompressible Renolds-averaged Navier-Stokes equations. We consider the case when the gas flows upwards. The equations are non-dimensionalised using $L_g = \mu_g/\sqrt{\rho_g T_w}$ as the length scale, where ρ_g, μ_g are the density and viscosity of the gas, respectively, and T_w is the magnitude of the shear stress along the wall for the case when the lower wall is flat. The velocity scale is chosen as the so-called friction velocity, $U_g = \sqrt{T_w/\rho_g}$. Besides, T_w is used as the scale for the pressure and the Reynolds stresses. Introducing the stream function Ψ and eliminating the pressure from the governing equations, we obtain

$$\nabla^4\Psi = -\frac{\partial(\Psi,\nabla^2\Psi)}{\partial(x,z)} - \mathscr{R}, \tag{1}$$

where

$$\nabla^2 = \partial_x^2 + \partial_z^2, \quad \nabla^4 = (\nabla^2)^2, \tag{2}$$

and

$$\frac{\partial(f,g)}{\partial(x,z)} = (\partial_x f)(\partial_z g) - (\partial_z f)(\partial_x g), \quad \mathscr{R} = \partial_{xz}\tau_{11} + \partial_z^2\tau_{12} - \partial_x^2\tau_{12} - \partial_{xz}\tau_{22}. \tag{3}$$

Here τ_{ij} are the components of the Reynolds stress tensor $\boldsymbol{\tau}$ due to random turbulent fluctuations in the gas momentum. The Cartesian coordinate system (x, z) is defined so that the x-axis points downwards along the interface (which is modelled as a solid wall for the gas problem). The z-axis points into the gas and is perpendicular to the x-axis. The undisturbed interface is given by $z = 0$.

In the case when the interface is flat, Eq. (1) reduces to

$$\Psi_0'''' = -\tau_{0\,12}'', \tag{4}$$

where Ψ_0 and $\boldsymbol{\tau}_0$ denote the stream function and the Reynolds stress tensor corresponding to the base flow, respectively. (It is assumed that Ψ_0 and $\tau_{0\,12}$ are functions of z only and that $\tau_{0\,11} = \tau_{0\,22} = 0$.) Using the mixing length model for $\tau_{0\,12}$,

$$\tau_{0\,12} = l^2\,|\Psi_0''|\,\Psi_0'', \quad l = \kappa z(1 - e^{-z/A}), \tag{5}$$

where $\kappa = 0.41$ is the von Kármán constant and $A = 25$ is the damping friction (See Ref. [47], p. 571), and noting that $\Psi'' < 0$ for the case when the gas flows upwards, we obtain the following equation:

$$\Psi_0'' = -\left(\frac{2(M - z)}{M + \sqrt{M^2 + 4l^2M(M - z)}}\right), \quad \Psi_0|_{z=0} = \Psi_0'|_{z=0} = 0, \tag{6}$$

under assumptions that the dimensionless shear stress is -1 at the flat interface, i.e. $\Psi_0''|_{z=0} = -1$ (this is due to the choice of scaling), and that the flow is symmetric with respect to the midplane of the channel, which implies $\Psi_0''|_{z=M} = 0$. Here, $2M$ is the dimensionless distance between the undisturbed liquid surface and the upper wall of the channel.

2.1.1. Flow over a wavy wall of small amplitude

For a wavy interface of small amplitude, i.e. when the interface at a particular time is given by $z = s(x) = \epsilon e^{i\alpha x}$, it has been verified in Ref. [24] that the use of the orthogonal boundary-layer coordinates first introduced by Benjamin [23] as

$$\xi = x - i\epsilon e^{-\alpha z}e^{i\alpha x}, \quad \eta = z - \epsilon e^{-\alpha z}e^{i\alpha x}, \tag{7}$$

is sufficient to obtain good agreement with experiments on turbulent gas flow over wavy wall [27]. With this approach, there is no need to introduce a model for waviness-induced Reynolds stresses and these stresses can be taken to be zero. One should note that in these coordinates the lower wall is, to first order in ϵ, given by $\eta = 0$.

We use the asymptotic expansion for Ψ as

$$\Psi^\alpha = \Psi_0(\eta) + \epsilon\,\Psi_1^\alpha(\eta)e^{i\alpha\xi} + O(\epsilon^2), \tag{8}$$

and assume that $\bar{\tau}_{11} = \bar{\tau}_{22} = 0$ and $\bar{\tau}_{12}(\eta) = \tau_{012}(\eta)$, where $\bar{\tau}_{ij}$ denote the components of $\boldsymbol{\tau}$ in the curvilinear coordinates (ξ, η). At first order we obtain

$$\begin{aligned}&\Psi_1^{\alpha\,\prime\prime\prime\prime} - (2\alpha^2 + i\alpha\,\Psi_0')\,\Psi_1^{\alpha\,\prime\prime} + (\alpha^4 + i\alpha^3\,\Psi_0' + i\alpha\,\Psi_0''')\,\Psi_1^\alpha\\ &= e^{-\alpha\eta}\left(-4\alpha\,\Psi_0'''' + 4\alpha^2\,\Psi_0''' + 2i\alpha^2\,\Psi_0'\,\Psi_0'' - 2\alpha\,\tau_{0\,12}'' - 2\alpha^2\,\tau_{0\,12}' + 4\alpha^3\,\tau_{0\,12}\right),\end{aligned} \tag{9}$$

and the boundary conditions are

$$\Psi_1^\alpha|_{\eta=0,\,M} = \Psi_1^{\alpha\prime}|_{\eta=0,\,M} = 0. \tag{10}$$

On the other hand, it can be shown that the shear stress and the normal stress imposed on the interface by the turbulent gas are

$$\tau_s(\alpha) = \Psi_1^{\alpha\prime\prime}(0) - 2\alpha, \quad \tau_n(\alpha) = -i\left[\frac{2}{M} + 2\alpha + \frac{1}{\alpha}\Psi_1^{\alpha\prime\prime\prime}(0)\right], \tag{11}$$

respectively. For each α, these stresses can be computed by numerically solving the boundary value problem, Eq. (9), and computing $\Psi_1^{\alpha\prime\prime}(0)$ and $\Psi_1^{\alpha\prime\prime\prime}(0)$.

Now, let the interface $s(x)$ be an arbitrary periodic function of period λ given by

$$y = s(x) = \sum_{\substack{k=-\infty \\ k\neq 0}}^{\infty} s_k \, e^{i\alpha_k x}, \tag{12}$$

where $\alpha_k = 2\pi k/\lambda$. Assuming that the perturbations to the shear stress $\widetilde{\mathscr{T}}$ and to the normal stress $\widetilde{\mathscr{N}}$ imposed by the turbulent gas on the interface depend linearly on the interface profile (which is equivalent to truncating Taylor series expansions at first order, i.e. taking linear approximations), we obtain

$$\widetilde{\mathscr{T}}[s(x)] = -1 + \sum_{\substack{k=-\infty \\ k\neq 0}}^{\infty} s_k \, \tau_s(\alpha_k) \, e^{i\alpha_k x}, \tag{13}$$

and

$$\widetilde{\mathscr{N}}[s(x)] = P_0(x) + \sum_{\substack{k=-\infty \\ k\neq 0}}^{\infty} s_k \, \tau_n(\alpha_k) \, e^{i\alpha_k x}, \tag{14}$$

where $P_0(x) = x/M + \text{const.}$ is the normal stress for the case when the interface is flat. Converting these into dimensional forms, we obtain that the tangential and normal stresses are given by

$$\overline{\mathscr{T}}\left[\sum_{\substack{k=-\infty \\ k\neq 0}}^{\infty} \bar{s}_k e^{i\bar{\alpha}_k \bar{x}}\right] = T_w \left(-1 + \sum_{\substack{k=-\infty \\ k\neq 0}}^{\infty} \frac{\bar{s}_k}{L_g} \, \tau_s(L_g \bar{\alpha}_k) \, e^{i\bar{\alpha}_k \bar{x}}\right), \tag{15}$$

and

$$\overline{\mathscr{N}}\left[\sum_{\substack{k=-\infty \\ k\neq 0}}^{\infty} \bar{s}_k e^{i\bar{\alpha}_k \bar{x}}\right] = T_w \left(\frac{\bar{x}}{L_g \, M} + \sum_{\substack{k=-\infty \\ k\neq 0}}^{\infty} \frac{\bar{s}_k}{L_g} \, \tau_n(L_g \bar{\alpha}_k) \, e^{i\bar{\alpha}_k \bar{x}}\right), \tag{16}$$

respectively, where $\bar{x}$ is the dimensional x-coordinate and $\bar{\alpha}_k = 2\pi k/\bar{\lambda}$ with $\bar{\lambda} = L_g \lambda$ denoting the dimensional interface period.

2.1.2. Analysis of the stresses at the wall: limiting cases

In order to compute the shear and normal stresses imposed by the turbulent gas on the interface, one has to solve numerically Eq. (9) for each Fourier mode, α. Once the function Ψ_1^α is obtained, the stresses are then given by Eq. (11). This procedure might be time-consuming, in particular if one wants to analyse the effect of computational domain on the solutions, the Fourier modes change with respect to the size of the domain and the stresses need to be re-evaluated. To overcome such a difficulty we try to analyse two limiting cases of Eq. (9), $\alpha \ll 1$ and $\alpha \gg 1$, and to obtain the approximation solution of Ψ_1^α so that the stresses can be evaluated more easily, at least in the limit where the approximation is valid.

Assuming that $\alpha \ll 1$, we can expand Ψ_1^α as a power series in α and split the real and imaginary parts as

$$\Psi_1^\alpha = \psi_r^0 + i\,\psi_i^0 + \alpha(\psi_r^1 + i\,\psi_i^1) + \alpha^2(\psi_r^2 + i\,\psi_i^2) + O(\alpha^3). \tag{17}$$

Collecting the leading-order terms in Eq. (9) we have

$$\psi_r^{0\prime\prime\prime\prime} = 0, \quad \psi_i^{0\prime\prime\prime\prime} = 0, \tag{18}$$

which, together with zero boundary conditions, leads to $\psi_r^0 = 0$ and $\psi_i^0 = 0$. The problem at first order is

$$\psi_r^{1\prime\prime\prime\prime} = -4\,\Psi_0{}^{\prime\prime\prime\prime} - 2\tau_{012}{}'' = -2\Psi_0{}^{\prime\prime\prime\prime}, \quad \psi_r^1(\eta = 0, M) = \psi_r^{1\prime}(\eta = 0, M) = 0, \tag{19}$$

which gives us

$$\psi_r^1 = -2\Psi_0 + \left[\left(\frac{-4}{M^3}\right)\Psi_0(M) + \left(\frac{2}{M^2}\right)\Psi_0{}'(M)\right]\eta^3 + \left[\left(\frac{6}{M^2}\right)\Psi_0(M) - \left(\frac{2}{M}\right)\Psi_0{}'(M)\right]\eta^2. \tag{20}$$

Besides, we find that $\psi_i^1 = 0$. As a result, we have

$$Re\left(\Psi_1^\alpha\right) = \alpha\,\psi_r^1 + O(\alpha^2), \quad Im\left(\Psi_1^\alpha\right) = O(\alpha^2), \tag{21}$$

where Re and Im are the real part and imaginary parts of the function, respectively.

To test the validity of the asymptotic result, in Fig. 1 we show the comparison between the function $Re\left(\Psi_1^\alpha\right)$ with its leading order approximation, $\alpha\,\psi_r^1$. The function Ψ_1^α is obtained by solving numerically Eq. (9) while the function ψ_r^1 is given by Eq. (20). It is found that the range for which the approximation is acceptable is rather small. The relative error for $\alpha = 10^{-5}$ is about 2% while for $\alpha = 10^{-4}$ the relative error already increases to 60%. The discrepancy might be improved by including higher order terms, a problem which we will look at in the future.

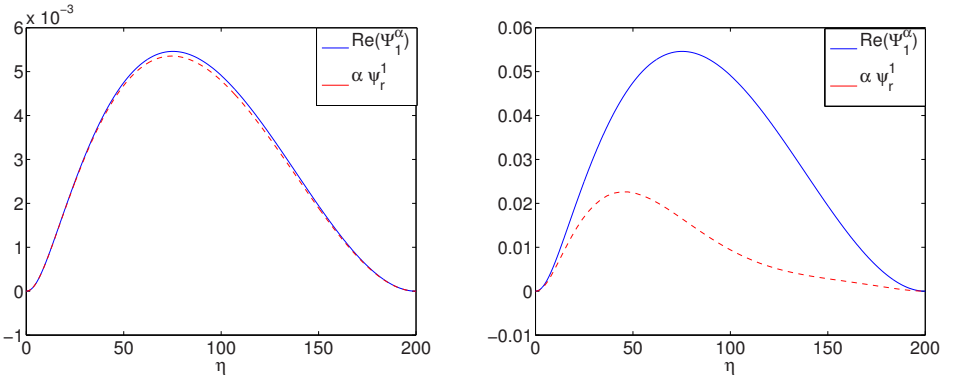

(a) $\alpha = 10^{-5}$ (b) $\alpha = 10^{-4}$

Fig. 1. (Color online) Comparison between function $Re(\Psi_1^\alpha)$ (solid blue curve) and its leading order approximation $\alpha\psi_r^1$ (dashed red curve) for (a) $\alpha = 10^{-5}$ and (b) $\alpha = 10^{-4}$.

On the other hand, for $\alpha \gg 1$, we first note that $e^{-\alpha\eta} \ll 1$ for $\eta = O(1)$. Therefore, the right-hand side of Eq. (9) is zero and we have $\Psi_1^\alpha(\eta = O(1)) = 0$. For $\eta = o(1)$, we make a rescaling by defining $y = \alpha\eta$ and assume $\Psi_1^\alpha(\eta) = 2\alpha\phi(y)$. Equation (9) can then be written as

$$\phi'''' - (2 + i\Psi_0{}')\,\phi'' + (1 + i\Psi_0{}' + i\Psi_0{}''')\,\phi = e^{-y}\left(-\Psi_0{}'''' + 3\,\Psi_0{}''' - 2\,\Psi_0{}'' - \frac{1-2y}{M\alpha^3} - \frac{2}{\alpha^2} + i\,\Psi_0{}'\,\Psi_0{}''\right). \tag{22}$$

Assume further that $\phi = h_r + ih_i$, we have,

$$h_r{}'''' - 2h_r{}'' + h_r + \frac{1}{\alpha^2} f h_i{}'' - \left(\frac{f}{\alpha^2} + \frac{1}{M\alpha^3}\right) h_i = \frac{2}{M\alpha^3}\,e^{-y}, \tag{23}$$

$$h_i{}'''' - 2h_i{}'' + h_i - \frac{1}{\alpha^2} f\,h_r{}'' + \left(\frac{1}{\alpha^2} f + \frac{1}{M\alpha^3}\right) h_r = \frac{1}{\alpha^4} f f'\,e^{-y}, \tag{24}$$

where we have used the fact

$$\frac{d\Psi_0}{dy} = \frac{1}{\alpha^2}\,f(y) + O\left(\frac{1}{\alpha^4}\right), \quad f(y) = -y + \frac{y^2}{2M\alpha}. \tag{25}$$

By observation, we can see that $h_r = O(1/\alpha^3)$ and $h_i = O(1/\alpha^4)$. The equations for the leading order terms are therefore

$$h_r'''' - 2h_r'' + h_r = \frac{2}{M\alpha^3}e^{-y}, \quad h_i'''' - 2h_i'' + h_i = \frac{y}{\alpha^4}\,e^{-y}. \tag{26}$$

It is found that

$$h_r = \frac{1}{4M\alpha^3}\,y^2e^{-y}, \quad h_i = \frac{1}{\alpha^4}\left(\frac{y^3}{24} + \frac{y^2}{8}\right)e^{-y}, \tag{27}$$

In sum, for $\alpha \gg 1$, we have

$$\Psi_1^\alpha \approx e^{-\alpha\eta}\left(\frac{\eta^2}{2M} + i\left(\frac{\eta^3}{12} + \frac{\eta^2}{4\alpha}\right)\right), \quad \Psi_1^{\alpha\prime\prime}(0) \approx \frac{1}{M} + \frac{i}{2\alpha}. \tag{28}$$

The comparison between the function Ψ_1^α and its approximation for $\alpha = 20$ is shown in Fig. 2. The agreement is fairly well.

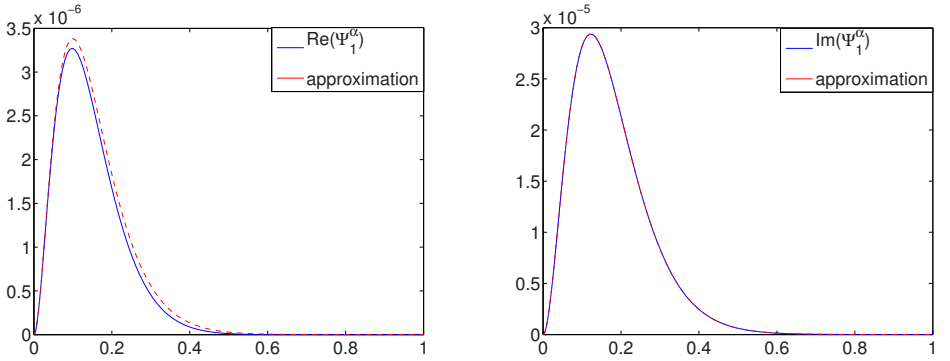

(a) $Re(\Psi_1^\alpha)$ (b) $Im(\Psi_1^\alpha)$

Fig. 2. (Color online) Comparison between the function Ψ_1^α (solid blue curve) and its leading order approximation (dashed red curve), Eq. (28), for $\alpha = 20$.

2.2. Liquid problem

The governing equations for the liquid flow are the incompressible Navier-Stokes equations:

$$\rho_l\,(\bar{\boldsymbol{u}}_{\bar{t}} + \bar{\boldsymbol{u}}\cdot\overline{\nabla}\bar{\boldsymbol{u}}) = -\overline{\nabla}\bar{p} + \mu_l\,\overline{\nabla}^2\bar{\boldsymbol{u}} + \rho_l\,\boldsymbol{g}, \quad \overline{\nabla}\cdot\bar{\boldsymbol{u}} = 0, \tag{29}$$

where $\bar{\boldsymbol{u}} = (\bar{u}, \bar{w})$ is the liquid velocity, $\bar{p}$ is the pressure, ρ_l and μ_l are the density and the viscosity of the liquid, respectively, $\boldsymbol{g} = (g\sin\theta, -g\cos\theta)$, g is the gravity and θ is the inclination angle of the channel, $\overline{\nabla} = (\partial_{\bar{x}}, \partial_{\bar{z}})^T$. The no-slip and no-penetration conditions at the wall require that

$$\bar{\boldsymbol{u}} = 0 \quad \text{at} \quad \bar{z} = 0. \tag{30}$$

Kinematic condition at the film surface requires that

$$\bar{w} = \bar{h}_{\bar{t}} + \bar{u}\bar{h}_{\bar{x}} \quad \text{at} \quad \bar{z} = \bar{h}(\bar{x}, \bar{t}), \tag{31}$$

where $\bar{h}$ is the thickness of the liquid film. Finally, the normal and tangential stress balance at the film surface require

$$\boldsymbol{n}\cdot\bar{\boldsymbol{\sigma}}\cdot\boldsymbol{n} = \gamma\kappa - \overline{\mathscr{N}}[\bar{h}], \quad \boldsymbol{t}\cdot\bar{\boldsymbol{\sigma}}\cdot\boldsymbol{n} = \overline{\mathscr{T}}[\bar{h}] \quad \text{at} \quad \bar{z} = \bar{h}(\bar{x}, \bar{t}), \tag{32}$$

where $\bar{\boldsymbol{\sigma}} = -\bar{p}\boldsymbol{I} + \mu_l(\overline{\nabla}\bar{\boldsymbol{u}} + \overline{\nabla}\bar{\boldsymbol{u}}^T)$ is the stress tensor of the liquid, $\boldsymbol{n}$ and $\boldsymbol{t}$ are the unit normal (pointing into the gas) and tangent vectors to the interface, respectively, γ is the surface tension coefficient and κ is the curvature of the

interface taken to be positive when the surface is concave downwards. In addition, $\mathscr{N}[\bar{h}]$ and $\mathscr{T}[\bar{h}]$ are the normal and tangential stresses, respectively, exerted onto the film surface by the turbulent gas that are found in the previous section.

Next, assuming long waves and using a systematic gradient expansion of the governing equations (e.g. Ref. [48]), we can derive the following long-wave evolution equation that is correct up to and including terms of $O(\epsilon)$, where $\epsilon \ll 1$ is the so-called long-wave or thin-film parameter that can be defined as the ratio of the undisturbed film thickness to the longitudinal length scale:

$$h_t + \partial_x \left[\frac{2}{3} h^3 - \frac{p_w}{2} h^2 + \epsilon \left(\left[\frac{8Re}{15} h^6 - \frac{2\cot\theta}{3} h^3 \right] h_x + \frac{Ca}{3} h^3 h_{xxx} - \frac{4Re\, p_w}{15} h^5 h_x + \frac{\nu p_w}{2} h^2 \mathscr{T}_1[h] \right) \right] = 0. \tag{33}$$

Here $h(x,t)$ is the dimensionless film thickness scaled by the undisturbed film thickness h_0, x is the dimensionless longitudinal coordinate scaled by h_0/ϵ, t is dimensionless time scaled by $h_0/(\epsilon U_l)$, where $U_l = \rho_l g h_0^2 \sin\theta / 2\mu_l$ is the Nusselt surface speed. The dimensionless parameters are the Reynolds number,

$$Re = \frac{\rho_l U L_l}{\mu_l}, \tag{34}$$

the scaled inverse capillary number,

$$Ca = \frac{\epsilon^2 \gamma}{\mu_l U}, \tag{35}$$

the scaled shear stress imposed by the gas on the undisturbed interface,

$$p_w = \frac{h_0 T_w}{\mu_l U_l}, \tag{36}$$

and the ratio of the length scales used to non-dimensionalise the liquid and gas problems, respectively,

$$\nu = \frac{h_0}{\epsilon L_g}. \tag{37}$$

In addition, the operator $\mathscr{T}_1$ is defined by

$$\mathscr{T}_1 \left[\sum_{\substack{k=-\infty \\ k\neq 0}}^{\infty} s_k e^{i\beta_k x} \right] = \sum_{\substack{k=-\infty \\ k\neq 0}}^{\infty} s_k \, \tau_s \left(\frac{\beta_k}{\nu} \right) e^{i\beta_k x}, \tag{38}$$

where $\beta_k = 2\pi k/\bar{\lambda}$ with $\bar{\lambda}$ denoting the period for the variable x.

2.3. Weakly nonlinear model

The weakly nonlinear model is derived using the following ansatz, with the rescaling of the spatial domain from $[-L, L]$ to a 2π-periodic one, $[-\pi, \pi]$:

$$h(x,t) = 1 + \epsilon \left(\frac{L}{\pi} \right) \left(\frac{1}{4 - p_w} \sqrt{\frac{3|D|^3}{Ca}} \right) H(X,T), \quad X = \left(\frac{\pi}{L} \right) \sqrt{\frac{3|D|}{Ca}} \left(x + (2 - p_w)t \right), \quad T = \left(\frac{\pi}{L} \right)^2 \frac{3\epsilon D^2}{Ca} t, \tag{39}$$

where

$$D = \frac{8Re}{15} - \frac{2\cot\theta}{3} - \frac{4Re\, p_w}{15}. \tag{40}$$

Equation (33) is then reduced, collecting only the leading order terms, to

$$H_T + HH_X \pm H_{XX} + \frac{\delta}{\sigma} \left(\mathscr{T}_1[H] \right)_X + \sigma^2 H_{XXXX} = 0, \tag{41}$$

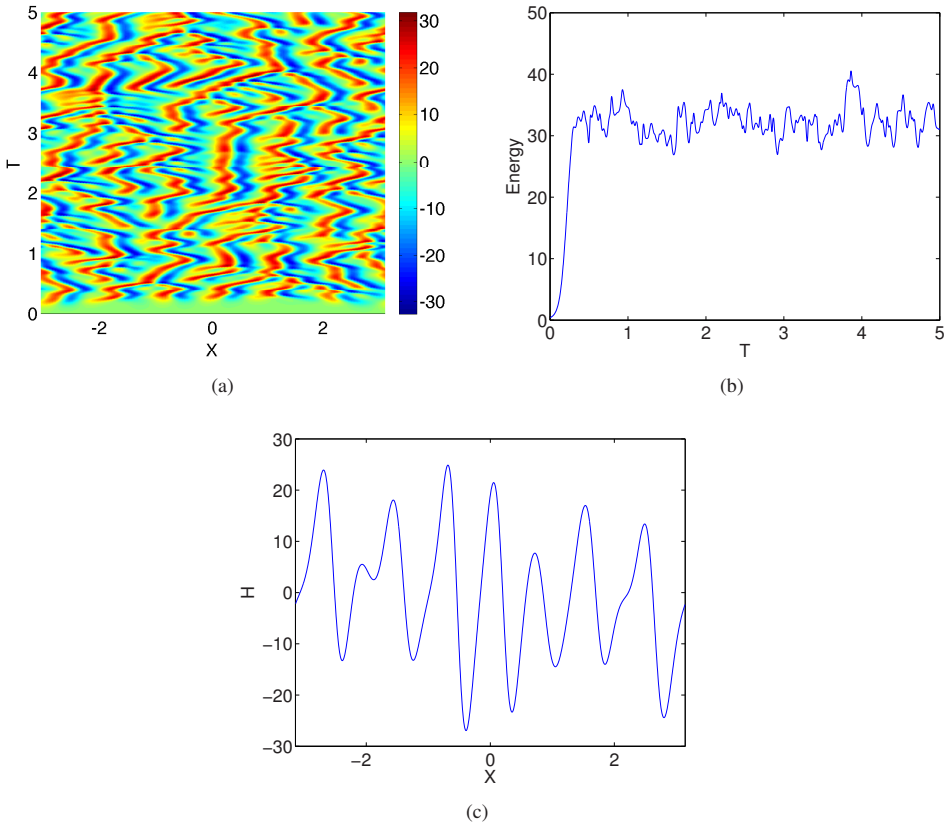

(a) (b) (c)

Fig. 3. (Color online) $\sigma = 0.1$, $\delta = 0$. The time evolution of the solution is shown in (a), the evolution of its corresponding energy is shown in (b) and the solution at $t = 5$ is shown in (c).

where H is of zero mean,

$$\sigma = \frac{\pi}{L}, \quad \delta = \frac{\nu p_w}{2}\sqrt{\frac{Ca}{3|D|^3}}, \tag{42}$$

and the $+/-$ sign corresponds to positive/negative value of D, respectively. Besides, we have

$$\mathscr{T}_1\left[\sum_{\substack{k=-\infty\\k\neq 0}}^{\infty} H_k e^{ikX}\right] = \sum_{\substack{k=-\infty\\k\neq 0}}^{\infty} H_k \tau_s\left(\sigma A\, k\right) e^{ikX}, \quad A = \frac{1}{\nu}\sqrt{\frac{3|D|}{Ca}}. \tag{43}$$

The final equation, Eq. (41), is the KS equation with an additional term contributed from the counter-current gas flow. There are three free parameters, σ, δ, A and the spatial domain is 2π-periodic.

3. Numerical investigation: Time dependent simulations

In this section we numerically investigate solutions of Eq. (41) using the implicit-explicit two-step backward differentiation formula presented in Ref. [42]. We use 124 Fourier modes in space and the time step is 0.001. The parameter A is fixed to be 1 so there are two free parameters in the problem. Besides, the initial condition is chosen as

$$H_0(X) = \frac{1}{10}\sum_{k=1}^{10}\left(\alpha_{1k}\cos(kX) + \alpha_{2k}\sin(kX)\right), \tag{44}$$

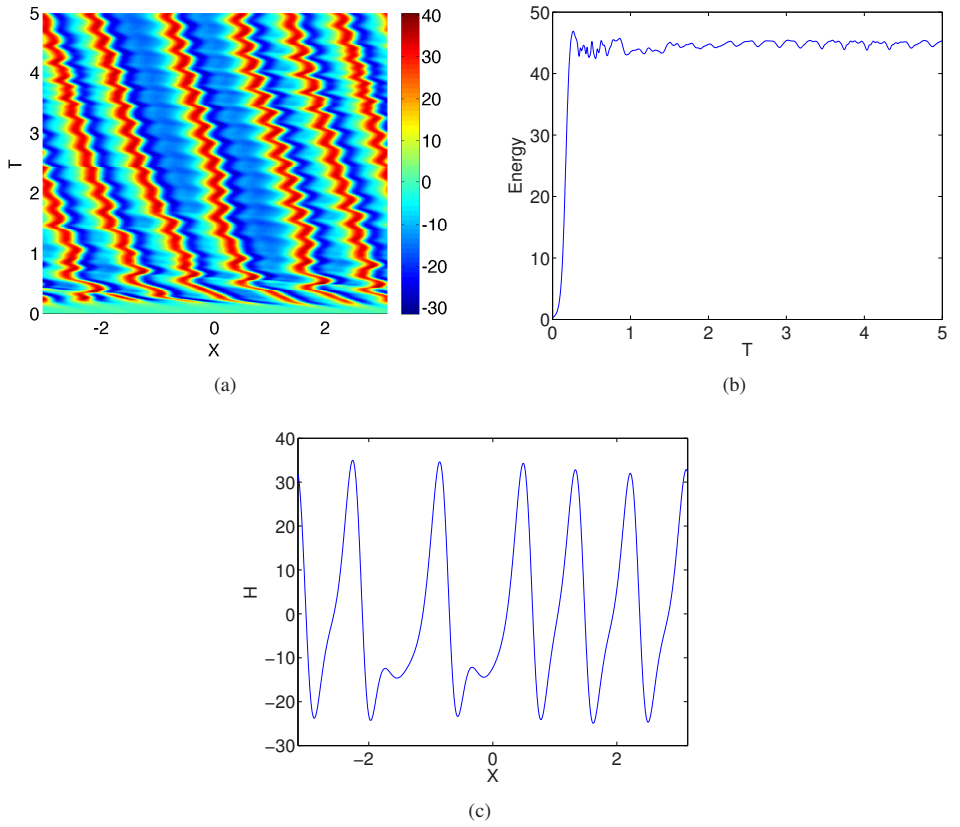

Fig. 4. (Color online) $\sigma = 0.1$, $\delta = 0.3$. The time evolution of the solution is shown in (a), the evolution of its corresponding energy is shown in (b) and the solution at $t = 5$ is shown in (c).

where the coefficients, α_{1k}, α_{2k}, $k = 1, \ldots, 10$, are chosen randomly in the interval $[0, 1]$. We also define an energy as the L^2-norm of the solution and use it as a verification of the attractor:

$$\sqrt{\int_{-\pi}^{\pi} H^2(X,T)dX}. \tag{45}$$

As noted earlier the solution of the KS equation ($\delta = 0$) exhibits temporal chaos for small σ. This is illustrated in Fig. 3 where the time evolution and the energy of the solution for $\sigma = 0.1$ are depicted. The solution pattern has no regular structure and nor does the energy. On the other hand, the counter-current turbulent gas might regularise the solution. In Fig. 4 we show the solution for $\sigma = 0.1$ and $\delta = 0.3$. Although it is still fluctuating, the solution approaches a localised structure and the deviation of the energy is much smaller. Indeed, if we increase the gas parameter δ further, as is shown in Fig. 5 for $\sigma = 0.1$ and $\delta = 1$, the solution evolves into a train of spatially periodic cellular structures, each of which approaching a solitary wave solution, as can be seen in Fig. 5(c) for the solution at $t = 5$.

An extensive test is performed in Table 1 for different values of the pertinent parameters. It is found that for $\delta = 1$ the solution always evolves to traveling pulses. Note that similar phenomena were observed previously for the generalised KS (gKS) equation where an additional dispersion term present in the form of H_{XXX}. The regularising effect of the dispersion term was studied in Refs. [43,44,45,46] and a rigorous coherent structure theory was developed to describe the interaction of solitary pulses. We believe that a similar approach can be extended to the present model and this will be fulfilled in the near future.

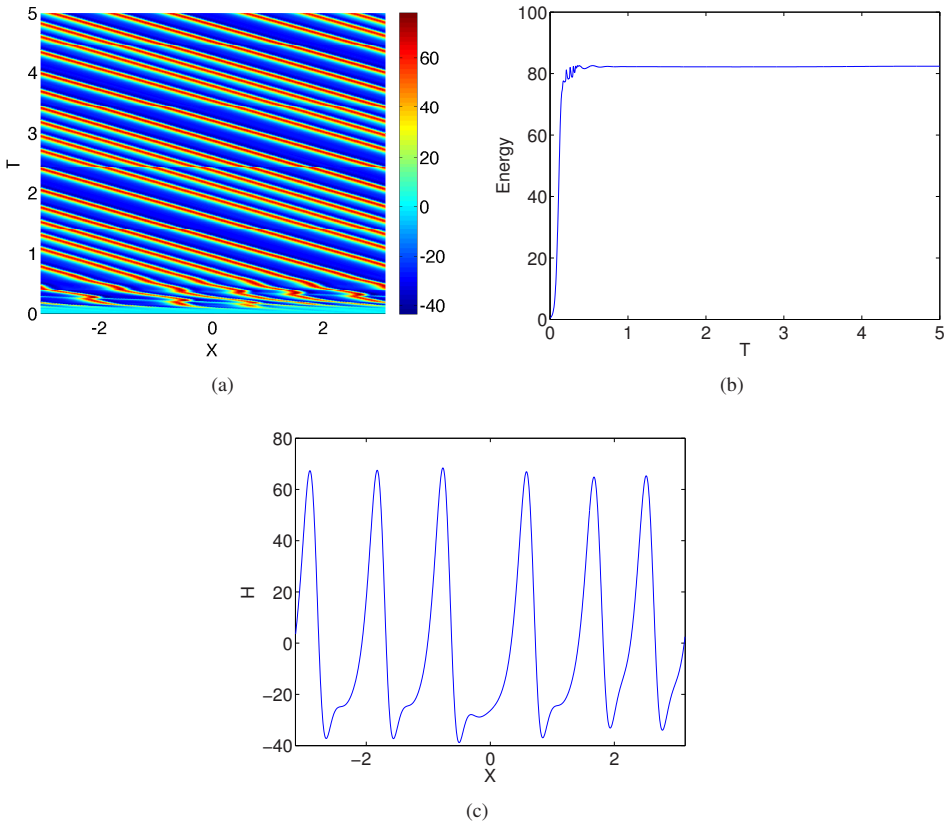

Fig. 5. (Color online) $\sigma = 0.1$, $\delta = 1$. The time evolution of the solution is shown in (a), the evolution of its corresponding energy is shown in (b) and the solution at $t = 5$ is shown in (c).

Table 1. Non-stationary attractors for different parameter values. The abbreviations are defined as following: chaos (CA); periodic pulses (PP); standing waves (SW); unimodal traveling waves (TW); periodic homoclinic burst (PH); zero state (ZS)

	$\sigma = 0.06$	$\sigma = 0.1$	$\sigma = 0.4$	$\sigma = 0.45$	$\sigma = 0.52$	$\sigma = 0.7$	$\sigma = 1$
$\delta = 0$	CA	CA	SW	PH	TW	SW	ZS
$\delta = 1$	PP	PP	PP	PP	TW	TW	TW

4. Conclusion

We have studied the dynamics of a thin liquid layer flowing under gravity down a planar inclined substrate in the presence of a counter-current turbulent gas. The model is the KS equation with an additional non-local term multiplied by a parameter representing the relative importance of the turbulent gas. The non-local term was derived in terms of Fourier coefficients and the function corresponding to each Fourier mode is obtained from a fourth-order boundary value problem.

Time dependent computations of the full non-local model reveal that the counter-current turbulent gas can regularise the dynamics of the usual spatio-temporal chaos of the KS equation in favour of regular trains of traveling pulses of approximately the same shape. Similar phenomena were observed with a gKS equation where an additional local dispersion term is present. It is therefore of interest to extend the previously developed coherent-structure theory for the gKS equation [43,44,45,46] to the non-local model considered here, and this is left as a topic for future research.

5. Acknowledgements

We are grateful to D. T. Papageorgiou for useful comments and discussions. We acknowledge financial support from EPSRC under grant EP/J001740/1.

References

[1] P. A. Semyonov, Flows of thin liquid films, J. Tech. Phys. (in Russian) 14 (1944) 427.
[2] F. P. Stainthorp, The effect of co-current and counter-current air flow on the wave properties of falling liquid films, Trans. Inst. Chem. Eng. 45 (1967) 372.
[3] A. E. Dukler, L. Smith, Two-phase interactions in countercurrent flow: studies of the flooding mechanism, Annual Report, NUREG/CR-0617, U.S. Nuclear Regulatory Commision, Washington, DC.
[4] S. C. Lee, S. G. Bankoff, Parametric effects on the onset of flooding in flat-plate geometries, Int. J. Heat Mass Transfer 27 (1984) 1691. doi:10.1016/0017-9310(84)90152-2.
[5] D. Moalem Maron, A. E. Dukler, Flooding and upward film flow in vertical tubes – II. Speculations on film flow mechanisms, Int. J. Multiphase Flow 10 (1984) 599. doi:10.1016/0017-9310(84)90152-2.
[6] K. W. McQuillan, P. B. Whalley, G. F. Hewitt, Flooding in vertical two phase flow, Int. J. Multiphase Flow 1 (6) (1985) 741–760. doi:10.1016/0301-9322(85)90022-9.
[7] T. K. Larson, C. H. Oh, J. C. Chapman, Flooding in a thin rectangular slit geometry representative of ATR fuel assembly side-plate flow channels, Nucl. Eng. Des. 152 (1994) 277. doi:10.1016/0029-5493(94)90092-2.
[8] S. Jayanti, A. Tokarz, G. F. Hewitt, Theoretical investigation of the diameter effect on flooding in countercurrent flow, Int. J. Multiphase Flow 22 (1996) 307. doi:10.1016/0301-9322(95)00069-0.
[9] Y. Sudo, Mechanisms and effects of predominant parameters regarding limitation of falling water in vertical counter-current two-phase flow, J. Heat Transf. 118 (1996) 715. doi:10.1115/1.2822691.
[10] A. Zapke, D. G. Kröger, Countercurrent gasliquid flow in inclined and vertical ducts – I: Flow patterns, pressure drop characteristics and flooding, Int. J. Multiphase Flow 26 (2000) 1439. doi:10.1016/S0301-9322(99)00097-X.
[11] A. Zapke, D. G. Kröger, Countercurrent gas-liquid flow in inclined and vertical ducts – II: The validity of the Froude-Ohnesorge number correlation for flooding, Int. J. Multiphase Flow 26 (2000) 1457. doi:10.1016/S0301-9322(99)00098-1.
[12] E. I. P. Drosos, S. V. Paras, A. J. Karabelas, Counter-current gas-liquid flow in a vertical narrow channel – Liquid film characteristics and flooding phenomena, Int. J. Multiphase Flow 32 (2006) 51. doi:10.1016/j.ijmultiphaseflow.2005.07.005.
[13] M. N. Pantzali, A. A. Mouza, S. V. Paras, Counter-current gas-liquid flow and incipient flooding in inclined small diameter tubes, Chem. Eng. Sci. 63 (2008) 3966. doi:10.1016/j.ces.2008.05.003.
[14] C. J. Shearer, J. F. Davidson, The investigation of a standing wave due to gas blowing upwards over a liquid film; its relation to flooding in wetted-wall columns, J. Fluid Mech. 22 (1965) 321.
[15] V. V. Guguchkin, E. A. Demekhin, G. N. Kalugin, E. E. Markovich, V. G. Pikin, Linear and nonlinear stability of combined plane-parallel flow of a film of liquid and gas, Fluid Dyn. 14 (1979) 26. doi:10.1007/BF01050808.
[16] E. A. Demekhin, Nonlinear waves in a liquid film entrained by a turbulent gas stream, Fluid Dyn. 16 (1981) 188. doi:10.1007/BF01090346.
[17] L. A. Jurman, M. J. McCready, Study of waves on thin liquid films sheared by turbulent gas flows, Phys. Fluids A 1 (1989) 522. doi:10.1063/1.857553.
[18] C.-A. Peng, L. A. Jurman, M. J. McCready, Formation of solitary waves on gas-sheared liquid layers, Int. J. Multiphase Flow 17 (1991) 767. doi:10.1016/0301-9322(91)90055-8.
[19] Y. Y. Trifonov, Counter-current gas-liquid wavy film flow between the vertical plates analyzed using the Navier-Stokes equations, AIChE J. 56 (2010) 1975. doi:10.1002/aic.12128.
[20] Y. Y. Trifonov, Flooding in two-phase counter-current flows: Numerical investigation of the gasliquid wavy interface using the NavierStokes equations, Int. J. Multiphase Flow 36 (2010) 549. doi:10.1016/j.ijmultiphaseflow.2010.03.006.
[21] Y. Y. Trifonov, Counter-current gas–liquid flow between vertical corrugated plates, Chem. Eng. Sci. 66 (2011) 4851. doi:10.1016/j.ces.2011.06.044.
[22] J. W. Miles, On generation of surface waves by shear flows, J. Fluid Mech. 3 (1957) 185.
[23] T. B. Benjamin, Shearing flow over a wavy boundary, J. Fluid Mech. 6 (1959) 161. doi:10.1017/S0022112059000568.
[24] D. Tseluiko, S. Kalliadasis, Nonlinear waves in counter-current gasliquid film flow, J. Fluid Mech. 673 (2011) 19. doi:10.1017/S002211201000618X.
[25] R. Vellingiri, D. Tseluiko, N. Savva, S. Kalliadasis, Dynamics of a liquid film sheared by a co-flowing turbulent gas, Int. J. Multiphase Flow 56 (2013) 93. doi:10.1016/j.ijmultiphaseflow.2013.05.011.
[26] C. B. Thorsness, P. E. Morrisroe, T. J. Hanratty, A comparison of linear theory with measurements of the variation of shear stress along a solid wave, Chem. Eng. Sci. 33 (1978) 579. doi:10.1016/0009-2509(78)80020-7.
[27] D. P. Zilker, G. W. Cook, T. J. Hanratty, Influence of the amplitude of a solid wavy wall on a turbulent flow. Part 1. Non-separated flows, J. Fluid Mech. 82 (1977) 29. doi:10.1017/S0022112077000524.
[28] V. Y. Shkadov, Wave flow regimes of thin layer of viscous fluid subject to gravity, Fluid Dyn. 2 (1967) 29. doi:10.1007/BF01024797.
[29] C. Ruyer-Quil, P. Manneville, Modeling film flows down inclined planes, Eur. Phys. J. B. 6 (1998) 277. doi:10.1007/s100510050550.
[30] P. Manneville, C. Ruyer-Quil, Improved modeling of flows down inclined planes, Eur. Phys. J. B. 15 (2000) 357. doi:10.1007/s100510051137.
[31] C. Ruyer-Quil, P. Manneville, Further accuracy and convergence results on the modeling of flows down inclined planes by weighted-residual approximations, Phys. Fluids 14 (1) (2002) 170. doi:10.1063/1.1426103.

[32] C. Ruyer-Quil, B. Scheid, S. Kalliadasis, M. G. Velarde, Thermocapillary long waves in a liquid film flow. Part 1. Low-dimensional formulation, J. Fluid Mech. 538 (2005) 199. doi:10.1017/S0022112005005422.
[33] B. Scheid, C. Ruyer-Quil, S. Kalliadasis, M. G. Velarde, R. K. Zeytounian, Thermocapillary long waves in a liquid film flow. Part 2. Linear stability and nonlinear waves, J. Fluid Mech. 538 (2005) 223. doi:10.1017/S0022112005005446.
[34] P. M. J. Trevelyan, B. Scheid, C. Ruyer-Quil, S. Kalliadasis, Heated falling films, J. Fluid Mech. 592 (2007) 295. doi:10.1017/S0022112007008476.
[35] A. Pereira, S. Kalliadasis, Dynamics of a falling film with solutal Marangoni effect, Phys. Rev. E 78 (2008) 036312. doi:10.1103/PhysRevE.78.036312.
[36] G. I. Sivashinsky, D. M. Michelson, On Irregular Wavy Flow of a Liquid Film Down a Vertical Plane, Prog. Theor. Phys. 63 (1980) 2112. doi:10.1143/PTP.63.2112.
[37] J. M. Hyman, B. Nicolaenko, The Kuramoto-Sivashinsky equation: A bridge between PDE'S and dynamical systems, Physica D 18 (1986) 113. doi:10.1016/0167-2789(86)90166-1.
[38] D. T. Papageorgiou, Y. S. Smyrlis, The route to chaos for the Kuramoto-Sivashinsky equation, Theoret. Comput. Fluid Dynamics 3 (1991) 15. doi:10.1007/BF00271514.
[39] Y. S. Smyrlis, D. T. Papageorgiou, Predicting chaos for infinite dimensional dynamical systems: the Kuramoto-Sivashinsky equation, a case study, Proc. Natl Acad. Sci. USA 88 (1991) 11129.
[40] T. Kawahara, Formation of saturated solitons in a nonlinear dispersive system with instability and dissipation, Phys. Rev. Lett. 51 (1983) 381. doi:10.1103/PhysRevLett.51.381.
[41] H.-C. Chang, E. A. Demekhin, D. I. Kopelevich, Laminarizing effects of dispersion in an active-dissipative nonlinear medium, Physica D 63 (1993) 299. doi:10.1016/0167-2789(93)90113-F.
[42] G. Akrivis, D. T. Papageorgiou, Y. S. Smyrlis, Computational Study of the Dispersively Modified Kuramoto-Sivashinsky Equation, SIAM J. Sci. Comput. 34 (2012) A792. doi:10.1137/100816791.
[43] C. Duprat, F. Giorgiutti-Dauphiné, D. Tseluiko, S. Saprykin, S. Kalliadasis, Liquid Film Coating a Fiber as a Model System for the Formation of Bound States in Active Dispersive-Dissipative Nonlinear Media, Phys. Rev. Lett. 103 (2009) 234501. doi:10.1103/PhysRevLett.103.234501.
[44] D. Tseluiko, S. Saprykin, C. Duprat, F. Giorgiutti-Dauphiné, S. Kalliadasis, Pulse dynamics in low-Reynolds-number interfacial hydrodynamics: Experiments and theory, Physica D 239 (2010) 2000. doi:10.1016/j.physd.2010.07.011.
[45] D. Tseluiko, S. Kalliadasis, Weak interaction of solitary pulses in active dispersive-dissipative nonlinear media, IMA J. Appl. Math. (2012) 1doi:10.1093/imamat/hxs064.
[46] M. Pradas, S. Kalliadasis, D. Tseluiko, Binary interactions of solitary pulses in falling liquid films, IMA J. Appl. Math. 77 (2012) 408. doi:10.1093/imamat/hxs028.
[47] H. Schlichting, K. Gersten, Boundary-Layer Theory, Springer, 2000.
[48] S. Kalliadasis, C. Ruyer-Quil, B. Scheid, M. G. Velarde, Falling liquid films, Springer Series on Applied Mathematical Sciences, London, 2012.